

## Unveiling Brain Region Patterns in PET/CT scans for Lung Cancer Assessment: A Computational AI Framework

Hakan Şat Bozcuk<sup>1\*</sup>, Ahmet Eren Şen<sup>2</sup>, Mehmet Artaç<sup>3</sup>, Buğra Kaya<sup>4</sup>

### Abstract

This study aims to investigate potential differences in brain activity between lung cancer patients and healthy controls at the time of diagnosis, utilizing a computer vision artificial intelligence (AI) model. Participants undergoing evaluation for lung cancer (cases) and with benign pulmonary nodules (controls) underwent Positron Emission Tomography/Computerized Tomography (PET/CT) scans. Specialized software reconstructed and labeled brain images. A computer vision AI model was developed using EfficientNet B0 through transfer learning, complemented by multivariate discriminant analysis. A total of 84 cases were recruited into the study. The constructed AI model exhibited robust accuracy (internal accuracy=1.0, external sensitivity=0.83) on a subset of cases (52 lung cancer patients, 22 controls). Notably, the right frontal lobe emerged as a crucial discriminator, displaying a 5% reduction in the ratio of frontal lobe to brainstem activity in lung cancer cases (Wilk's Lambda=0.877, P=0.002). Based solely on PET/CT brain imaging data, our AI model accurately classified lung cancer patients. The distinct role of the right frontal lobe in this study underscores the broader significance, shedding light on brain function disparities at lung cancer diagnosis.

**Keywords:** Lung Cancer; Pet/Ct; Artificial Intelligence.

### Introduction

The intricate communication between cancer cells and infiltrating neural cells is acknowledged [1]. However, it remains unclear whether such a connection exists between cancer cells and brain neural cells. An extensive body of literature highlights the potential impact of cancer treatments and associated conditions on the brain function of cancer patients. Yet, the precise relationship between brain functions and cancer development during the diagnostic phase remains elusive [2, 3]. Theoretically, given that cancer development and progression disrupt and modify the mechanisms governing nervous system development and regeneration, the nervous system could play a pivotal role in various aspects of cancer. Moreover, the reciprocal relationship between cancer and its therapies, with the potential to reshape the nervous system, introduces the possibility of neurological dysfunction or even malignancy development [4]. Conversely, it is plausible that brain dysfunction might contribute to the progression of cancer. Consequently, investigating the presence of any brain dysfunction at the time of cancer diagnosis, even prior to the initiation of treatment and any potential treatment-induced brain damage, holds significant importance in order to enhance our understanding of the intricate association between brain functions and cancer development. Artificial intelligence (AI) models for image classification have demonstrated

### Affiliation:

<sup>1</sup>Department of Medical Oncology, Medical Park Hospital, Antalya 07230, Turkey

<sup>2</sup>Department of Nuclear Medicine, Konya City Hospital, Konya 42020, Turkey

<sup>3</sup>Department of Medical Oncology, Necmettin Erbakan University Hospital, Konya 42090 Turkey

<sup>4</sup>Department of Nuclear Medicine, Necmettin Erbakan University Hospital, Konya 42090, Turkey

### \*Corresponding author:

Hakan Şat Bozcuk, Department of Medical Oncology, Medical Park Hospital, Antalya 07230, Turkey.

**Citation:** Hakan Şat Bozcuk, Ahmet Eren Şen, Mehmet Artaç, Buğra Kaya. Unveiling Brain Region Patterns in PET/CT scans for Lung Cancer Assessment: A Computational AI Framework. *Journal of Cancer Science and Clinical Therapeutics*. 7 (2023): 179-185.

**Received:** September 10, 2023

**Accepted:** September 21, 2023

**Published:** October 09, 2023

remarkable success in various medical contexts, including the assessment of brain tumors via magnetic resonance imaging (MRI), analysis of blood leucocyte images, diverse medical imaging modalities, lung computed tomography (CT) scans, skin lesion evaluations, and breast cancer histological images [5-11]. While Positron Emission Tomography / Computerized Tomography (PET / CT) scans are widely utilized in oncology to monitor cancer occurrence and progression, their sensitivity in detecting cranial metastasis remains limited. In contrast, PET scans have proven valuable in elucidating the functions of brain centers in various conditions, including depression [12, 13]. A plethora of pretrained computer vision models, such as Efficient-Net, Inception, ResNet, MobileNet, NasNet, and VGG, are available. Fine-tuning these models with additional training images has been shown to enhance their accuracy [14-20]. These models, once suitably trained, can be harnessed for diverse tasks, spanning from medical diagnostics to general applications like facial recognition, road lane detection, and vehicle license plate recognition [21]. Accordingly, our study follows a similar methodology. In light of these considerations, our study endeavors to leverage artificial intelligence techniques to detect discernible patterns of brain activity in patients diagnosed with lung cancer and healthy controls at the point of diagnosis. Furthermore, we delve into identifying the brain centers that wield the greatest significance in the intricate interplay between brain function and cancer development.

## Methods and Materials

### Recruitment of Patients and Controls

Participants diagnosed with lung cancer, with or without a confirmed pathological diagnosis, and who had undergone PET/CT scans at the time of diagnosis, were enrolled in the study. Both Non-Small Cell Lung Cancer (NSCLC) and Small Cell Lung Cancer (SCLC) pathologies were considered. Additionally, patients with benign lung nodules undergoing diagnostic evaluation were included. Both lung cancer patients and healthy controls with benign nodules were assessed at Necmettin Erbakan University's Medical Oncology and Nuclear Medicine Departments. Data spanning from September 20, 2022, to April 21, 2023, were retrieved from the hospital image database. Exclusion criteria encompassed cerebral metastatic disease on PET/CT, conditions impacting brain function (e.g., active psychiatric illness, addiction, organ failure), history of cerebrovascular events or brain surgery, and uncontrolled Diabetes Mellitus. Ethical approval was obtained from the Necmettin Erbakan University Ethical Committee.

### Brain PET/CT Image Reconstruction

Routine PET/CT imaging was performed using F18-FDG doses ranging from 7 to 12 mCi on the Siemens Biograph 6 True Point PET/BT scanner. The Syngo Via software and

MI neurology program, incorporating automated anatomical labeling, were employed [22]. This facilitated calculation of specific SUV mean outputs for various brain regions, including total brain, brain stem, bilateral frontal lobes, and multiple other regions (inferior frontal gyrus opercular, orbital, triangular, middle frontal gyrus and orbital area, superior frontal gyrus orbital, medial orbital, medial and dorsolateral area, supplementary motor area, precentral gyrus, temporal lobe, superior, middle, inferior temporal gyri, insula, fusiform gyrus, hippocampus, parahippocampus, amygdala, parietal lobe, superior parietal gyrus, supramarginal and angular gyri, inferior parietal gyrus (except supramarginal and angular gyri), postcentral gyrus, cerebellar hemi-spheres, thalamus, caudate nucleus, putamen, pallidum, cingulate and paracingulate gyri).

### Development and Testing of Computer Vision AI Model

The EfficientNet B0 pretrained model was fine-tuned in Google Collab Pro Medium via transfer learning. This process involved appending a sequential dense layer to the feature extractor, followed by a final dense layer with sigmoid activation for classification [14]. While other models like EfficientNet B3 and B7, Inception V3, ResNet V2, and MobileNet V2 were considered, EfficientNet B0 demonstrated superior accuracy during experimentation. The model was trained for 12 epochs, utilizing a learning rate of 0.001 and binary cross-entropy as the loss function. Post-training, the model's accuracy and loss curves were visualized using the Matplotlib library [23]. Additional libraries, including NumPy, TensorFlow, and Keras, were employed for model development [24-26]. To enhance the pretrained model's performance, sequential dense layers were introduced, augmenting the neural network. These layers connect each neuron (or unit) to all neurons in the preceding layer [27]. For a clearer understanding of the computer vision AI algorithm's functionality, regions of focus within brain PET/CT images were depicted using heatmaps and explainable artificial intelligence (XAI) views, facilitated by the Why library [28].

### Discriminant Analysis of Brain Functions

Exploration of brain regions potentially linked to lung cancer development commenced with univariate discriminant analysis. Given the numerous brain regions and their functions (both raw and as a ratio of brain stem activity), univariate tests were iterated around 200 times. A significance threshold of  $P < 0.20$  guided the selection of features for inclusion in the multivariate stage. Bonferroni correction, employing a  $P$  value of  $0.20/200$ , mandated a modified significance level of 0.001 or lower for the univariate tests [29]. In the multivariate discriminant analysis, significance was determined using tolerance and Wilk's Lambda, with a  $P$  value  $< 0.05$  considered statistically significant.

## Results

### General Characteristics:

The study encompassed a total of 84 participants (57 lung cancer patients and 27 healthy controls). The construction of the computer vision AI model utilized data from 74 cases with technically sufficient reconstructed brain image data (52 lung cancer patients and 22 healthy controls). The median age of the entire cohort was 62.5, with 80% of the cases representing male participants. Among the lung cancer group, the prevailing pathology observed was Squamous Non-Small Cell Lung Cancer (NSCLC), accounting for 51% of cases. For details, please refer to Table 1.

### Computer Vision Artificial Intelligence Model

The AI model was rooted in the pretrained EfficientNet B0 model, refined through fine-tuning using multiple brain/CT images from each of the 74 cases. In addition to the feature extractor layer, two sequential dense neural network layers were integrated into the model. A succinct summary of the

**Table 1:** Patient and Healthy Control Characteristics

	Lung Cancer	Heathy	Total
N (%)	57 (68)	27 (32)	84 (100)
Age (Median (Min-Max))	63 (47-85)	61 (24-75)	62.5 (24-85)
Gender			
Male (%)	90	59	80
Female (%)	10	41	20
Pathology			
Squamous NSCLC (%)	51	n/e	n/e
Non-Squamous NSCLC (%)	23	n/e	n/e
Small Cell Lung Cancer (%)	16	n/e	n/e

**Table 2:** Computer vision Artificial Intelligence Model Summary

Model: "sequential"

Layer (type)	Output Shape	Param #
my_efficientnet_b0 (KerasLayer)	(None, 1280)	4049564
dense (Dense)	(None, 256)	327936
dense_1 (Dense)	(None, 2)	514

=====  
 Total params: 4,378,014  
 Trainable params: 4,335,998  
 Non-trainable params: 42,016

model's architecture is available in Table 2. The compilation of AI model images from each case encompassed axial, coronal, and sagittal views, along with right lateral, left lateral, anterior, posterior, superior, inferior, right medial, and left medial views, culminating in a total of 11 views per case. For a visual understanding of the image types employed in the model, please consult Figure 1.

Figure 1a showcases the baseline images, while Figure 1b illustrates the heat map view, delineating crucial areas for classification. Furthermore, Figure 1c offers an example of the explainable artificial intelligence (XAI) view, highlighting pivotal regions for the AI model's construction. Following 12 training rounds (epochs), the model achieved an accuracy of 1.00 and a loss of 0.14. However, within the validation set, which constituted 20% of the training dataset, accuracy and loss figures stood at 0.64 and 3.26, respectively. Comprehensive insights into the AI model's training and loss curves are elucidated in Figure 2. Employing a distinct set of brain images from six lung cancer patients and healthy controls, the model accurately predicted the labels for five cases (sensitivity=0.83).

### Discriminant Analysis of Brain Functions between Lung Cancer Patients and Healthy Controls

Accounting for the Bonferroni correction-defined significance thresh-old of  $P \leq 0.001$ , the univariate discriminant analysis unveiled four significant brain regions. These encompassed the right frontal lobe, left frontal lobe, right frontal opercular area, and right middle frontal gyrus. Additionally, gender emerged as the fifth significant feature within the univariate analysis. Adopting a stepwise approach in multivariate discriminant analysis, solely the right frontal lobe and gender retained their significance out of the four brain regions and gender. For the right frontal lobe, the P value stood at 0.002, Wilk's Lambda registered at 0.877, and the tolerance figure reported as 0.955. For comprehensive insights into the discriminant analysis, consult Table 3, while significant associations within the univariate and multivariate tests are expounded in Figure 3 and Figure 4.

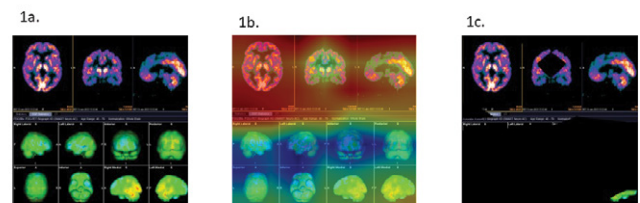


Figure 1a. Baseline PET / CT scan findings for the brain regions in a patient with lung cancer. Figure 1b. Heat map view of the same patient; showing areas of importance in classification process of the model. Figure 1c. XAI (explainable artificial intelligence) view of the same patient, again showing areas of note for the artificial intelligence model.

**Figure 1:** PET/CT scans findings for the brain regions in lung cancer cases and controls

Figure 2a. Loss curves

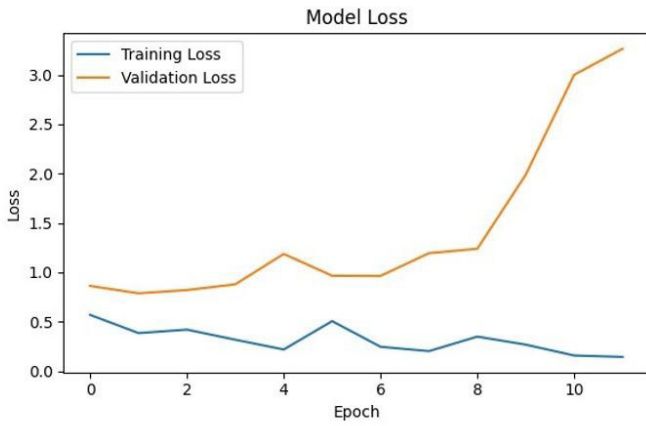


Figure 2b. Accuracy curves

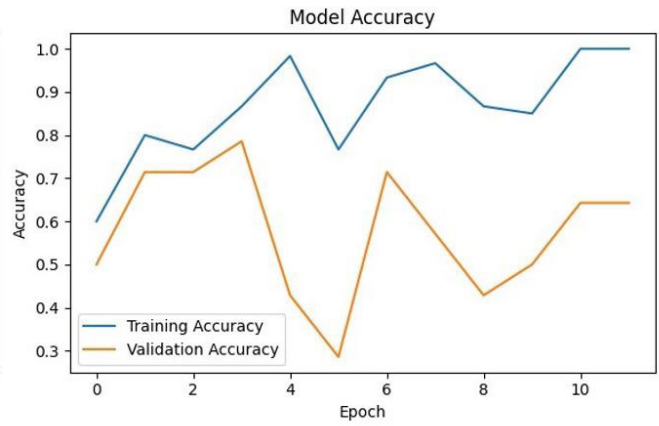


Figure 2: Loss and accuracy curves of the computer vision model

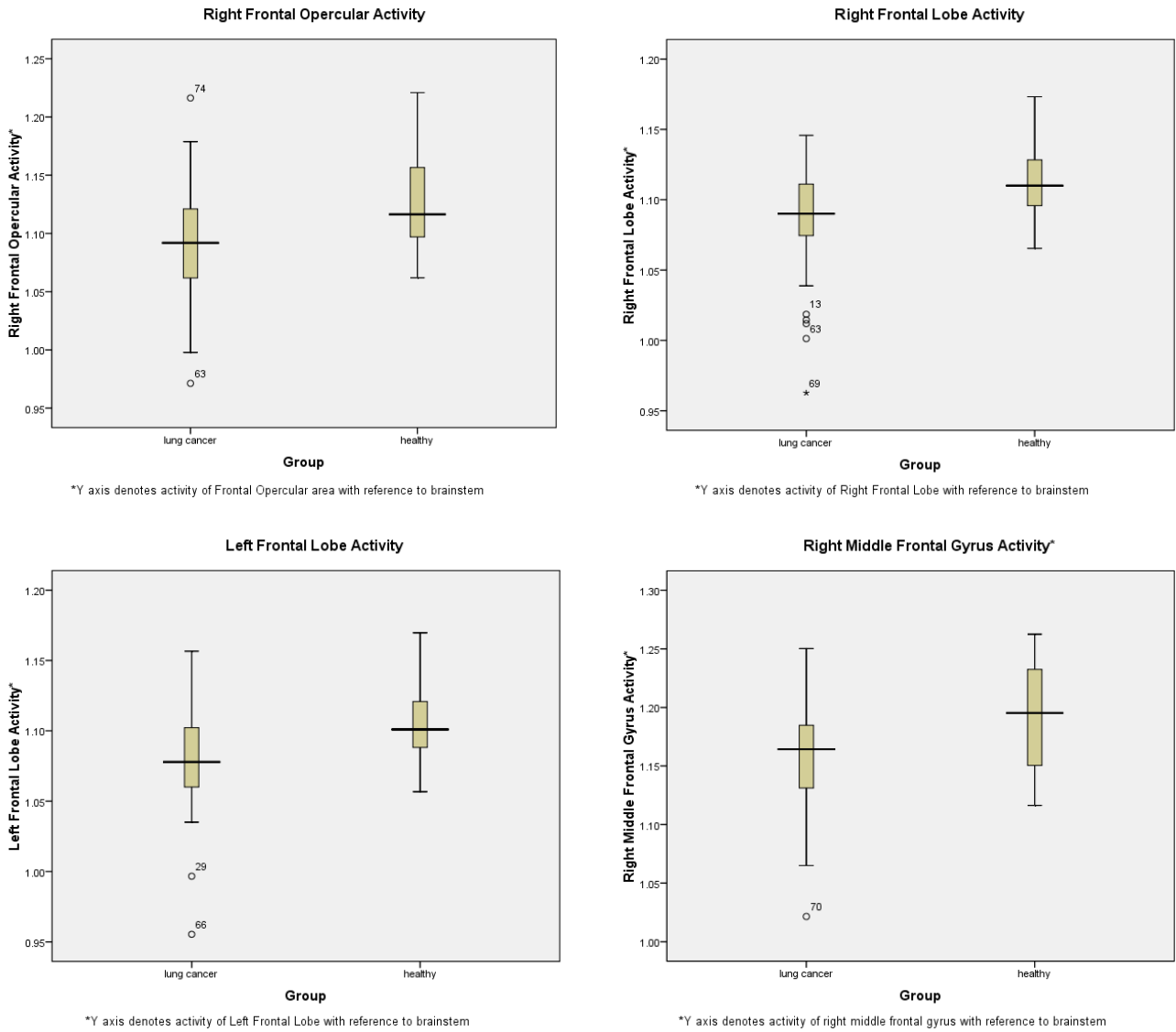
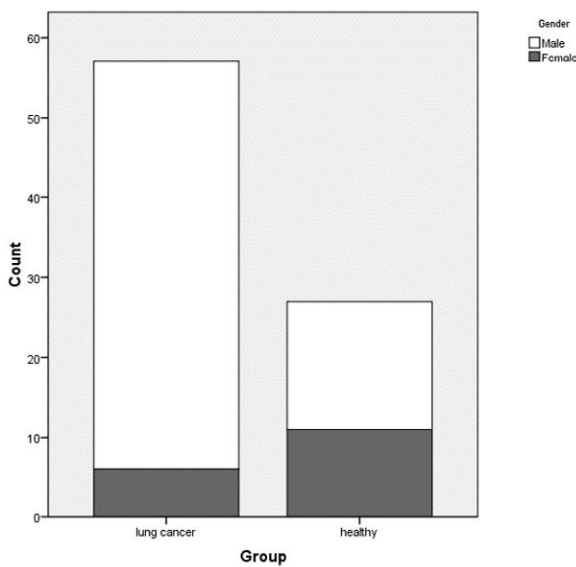


Figure 3: Activity of selected brain regions on PET / CT with and without lung cancer

**Table 3:** Analysis of patient features and brain regions with significant activity in cases with lung cancer and healthy controls

Feature or Brain Region	Univariate Discriminant Analysis				Multivariate Discriminant Analysis		
	Wilk's Lambda	Chi-square	df	P value	Tolerance	Wilk's Lambda	P value
Gender	0.877	10.729	1	0.001	0.995	0.864	0.005*
Right Frontal Lobe	0.864	11.932	1	0.001	0.995	0.877	0.002*
Left Frontal Lobe	0.883	10.177	1	0.001	0.6	0.775	0.376
Right Frontal Opercular Area	0.874	10.981	1	0.001	0.736	0.746	0.05
Right Middle Frontal Gyrus	0.869	11.454	1	0.001	0.403	0.765	0.186

\*; Selected by the stepwise method as statistically significant



**Figure 4:** Gender Distribution

## Discussion

Our study substantiates the presence of functional discrepancies within specific brain regions, as evidenced by PET/CT evaluations, in lung cancer patients at the point of diagnosis, even before any therapeutic interventions are initiated. Interestingly, through a focused analysis of concealed brain functions, our AI model effectively distinguishes between lung cancer patients and healthy controls. This finding is poised to illuminate the intricate connections between the nervous system and cancer. The exploration of whether this communication is facilitated or amplified by the immune system, as observed in the neuro immune oncology framework, and the potential temporal relationship between changes in brain function and cancer development stand as pivotal questions that warrant further investigation. A key contributor to the distinct functional profiles of brain regions in lung cancer patients and healthy controls could potentially be linked to the hypoactivity of

the right frontal lobe. Our findings revealed a lower right frontal to brainstem activity ratio in lung cancer patients compared to healthy controls. The right frontal lobe holds significant functions; while the right hemisphere plays a role in non-verbal abilities, the left hemisphere is involved in controlling language-related movement. Notably, frontal lobe damage frequently manifests as challenges in processing environmental feedback. This encompasses behaviors such as perseveration, risk-taking, non-compliance with rules, and impaired associative learning—all of which can stem from frontal lobe dysfunction [30]. Exploring whether these difficulties are more prevalent in the cancer population compared to healthy controls during cancer diagnosis is an avenue worth investigating. Furthermore, discerning whether these behavioral and neurological changes merely accompany the cancer development process or play an active role in influencing or being influenced by cancer development is of interest. The evolution of medicine recently is undeniably intertwined with the rise of AI [31]. Our study underscores the feasibility of constructing robust AI models utilizing visual data from PET/CT brain images. To our knowledge, this is one of the pioneering instances of a correlative AI study within the cancer population utilizing brain PET/CT data. Other AI investigations focusing on the brain have primarily employed different imaging modalities, such as brain MRI, to address varied needs. For example, the synergy of AI technology has notably enhanced the utility of MRI imaging [32]. However, our study underscores the potential of PET/CT brain images to offer critical insights into brain region functionality in cancer patients. While we believe our findings present significant contributions, limitations exist, with the most notable being the relatively modest sample size. Recognizing that computer vision AI models thrive with larger sample sizes, we acknowledge the possibility of missing certain patterns in our model [33]. Moreover, external images are imperative to fully gauge the utility of the model. Diversifying our patient pool to encompass other common cancers could shed light on whether the functional patterns observed in our brain regions are universally applicable. Notwithstanding these limitations, we believe that

our findings hold sufficient strength to spur the formulation of novel hypotheses. In essence, our study demonstrates that lung cancer patients' manifest distinct patterns of brain function compared to healthy controls, discernible at the time of diagnosis. Notably, the activity of the right frontal lobe emerges as a pivotal factor in this divergence. The ability of our AI model to accurately categorize cases within the lung cancer group or healthy controls underscores its clinical potential. Yet, further investigations are imperative to fully elucidate the interplay between the nervous system and cancer in our findings.

## Conclusions

At the time of diagnosis, before receiving any treatment, lung cancer patients have a different brain function pattern that is identifiable by an artificial intelligence model. The diminished right frontal lobe activity may be one of the fundamental components of this different brain function pattern seen in lung cancer patients.

## Author Contributions

Hakan Şat Bozcuk; found the study question, designed the study, analysed the study, wrote the paper. Ahmet Eren Şen; Collected the data, revised the paper. Mehmet Artaç; co designed the study, revised the paper. Buğra Kaya; Participated in data collection, also revised the paper.

## Funding

This research received no external funding.

## Institutional Review Board Statement

The study was conducted in accordance with the Declaration of Helsinki, and approved by the or Ethics Committee of Necmettin Erbakan University in 2022.

## Informed Consent Statement

"Informed consent was obtained from all subjects involved in the study".

Written informed consent for publication must be obtained from participating patients who can be identified (including by the patients themselves). Please state "Written informed consent has been obtained from the patient(s) to publish this paper" if applicable.

## Data Availability Statement

Data is unavailable due to privacy or ethical restrictions. Unidentifiable numerical patient data in tabular format is available upon request.

## Acknowledgments

We thank Levent Çapan, for being an inspiration for the study.

## Conflicts of Interest

The authors declare no conflict of interest.

## References

1. Silverman DA, Martinez VK, Dougherty PM, et al. Cancer-Associated Neurogenesis and Nerve-Cancer Cross-talk. *Cancer Res* 81 (2021): 1431-1440.
2. Kesler SR, Sleurs C, McDonald BC, et al. Brain imaging in pediatric cancer survivors: correlates of cognitive impairment. *J Clin Oncol* 39 (2021): 1775–1785.
3. McDonald BC. Structural neuroimaging findings related to adult non-CNS cancer and treatment: Review, integration, and implications for treatment of cognitive dysfunction: Review. *Neurotherapeutics* 18 (2021): 792-810.
4. Winkler F, Venkatesh HS, Amit M, et al. Cancer neuroscience: State of the field, emerging directions. *Cell* 186 (2023): 1689-1707.
5. Sultan HH, Nancy MS, Al-Atabany W. Multi-Classification of Brain Tumor Images Using Deep Neural Network. *IEEE Access* 7 (2019): 69215-69225.
6. Anaraki AK, Ayati M, Kazemi F. Magnetic resonance imaging-based brain tumor grades classification and grading via convolutional neural networks and genetic algorithms. *Biocybernetics and Biomedica Engineering* 39 (2019): 63-74.
7. Hasan AM, Jalab HA, Meziane F, et al. Combining Deep and Handcrafted Image Features for MRI Brain Scan Classification. *IEEE Access* 7 (2019): 79959-79967.
8. Liang G, Hong H, Xie W, et al. Combining Convolutional Neural Network with Recursive Neural Network for Blood Cell image classification. *IEEE Access* 6 (2018): 36188-36197.
9. Srivastava V, Purwar RK. Classification of CT Scan Images of Lungs Using Deep Convolutional Neural Network with External Shape-Based Features. *J Digit Imaging* 33 (2020): 252-261.
10. Mahbod A, Schaefer G, Wang C, et al. Skin Lesion Classification Using Hybrid Deep Neural Networks. *ICASSP* (2019).
11. Anupama MA, Sowmya V, Soman K. Breast Cancer Classification using Capsule Network with Preprocessed Histology Images. *ICCSP* (2019).
12. Chan TK, Li WI, Lau JHYH, et al. The diagnostic performance of 18 fluorine-fluorodeoxyglucose PET for brain metastases: a systematic review and meta-analysis. *Nucl Med Commun* 44 (2023): 741-749.

13. Sankar A, Melin A, Lorenzetti V, et al. A systematic review and meta-analysis of the neural correlates of psychological therapies in major depression. *Psychiatry Res Neuroimaging* 279 (2018): 31-39.
14. Tan M, Le QV. EfficientNet: Rethinking Model Scaling for Convolutional Neural Networks (2020). DOI: <https://doi.org/10.48550/arXiv.1905.11946>.
15. Szegedy C, Liu W, Jia Y, et al. Going Deeper with Convolutions (2014). arXiv:1409.4842 2014; DOI: <https://doi.org/10.48550/arXiv.1409.4842>.
16. He K, Zhang X, Ren S, et al. Deep Residual Learning for Image Recognition. *CVPR* (2016). DOI: 10.1109/CVPR.2016.90.
17. Howard AG, Zhu M, Chen B, et al. MobileNets: efficient convolutional neural networks for mobile vision applications (2017). arXiv:1704.04861 2017; DOI: <https://doi.org/10.48550/arXiv.1704.04861>.
18. Zoph B, Vasudevan V, Shlens J, et al. Learning Transferable Architectures for Scalable Image Recognition (2023). arXiv:1707.07012v4 2018; at <https://arxiv.org/pdf/1707.07012.pdf>. Accessed at 23.7.2023.
19. Simonyan K, Zisserman A. Very Deep Convolutional Networks for large-scale image recognition 6 (2015). arXiv:1409.1556v6 2015; DOI: <https://doi.org/10.48550/arXiv.1409.1556>.
20. Model fine tuning (2023). [https://clemsonciti.github.io/rcde\\_workshops/pytorch\\_advanced/03\\_finetune\\_pretrained\\_models.html](https://clemsonciti.github.io/rcde_workshops/pytorch_advanced/03_finetune_pretrained_models.html). Accessed at 8/18/2023.
21. 15 Computer Visions Projects You Can Do Right Now (2023). <https://neptune.ai/blog/15-computer-visions-projects>. Accessed at 8/18/2023
22. Fahmi R, Platsch G. Syngo.via database comparison in MI Neurology (2023). <https://www.siemens-healthineers.com/tr/molecular-imaging/mi-clinical-corner/whitepapers/syngo-via-database-comparison-in-mi-neurology>. Accessed at 8/19/2023.
23. Matplotlib: Visualization with Python (2023). <https://matplotlib.org>. Accessed at 8/19/2023
24. NumPy (2023). <https://numpy.org>. Accessed at 8/19/2023
25. Create production-grade machine learning models with TensorFlow (2023). <https://www.tensorflow.org>. Accessed at 8/19/2023
26. Keras (2023). <https://keras.io>. Accessed at 8/19/2023
27. Verma Y. A complete understanding of dense layers in neural networks (2023). <https://analyticsindiamag.com/a-complete-understanding-of-dense-layers-in-neural-networks>. Accessed at 8/19/2023.
28. Sayıcı MB. Why. Framework-agnostic XAI Library for Computer Vision, for understanding why models behave that way (2023). <https://github.com/mburaksayici/Why>. Accessed at 8/19/2023.
29. The Bonferroni Correction Method Explained (2023). [https://toptipbio.com/bonferroni-correction-method/#google\\_vignette](https://toptipbio.com/bonferroni-correction-method/#google_vignette). Accessed at 8/19/2023.
30. Centre for neuro skills. Frontal lobes (2023). <https://www.neuroskills.com/brain-injury/frontal-lobes/#:~:text=The%20left%20frontal%20lobe%20is,involved%20in%20nearly%20all%20behavior>. Accessed at 8/19/2023.
31. Beam AL, Drazen JM, Kohane IS, et al. Artificial Intelligence in Medicine. *N Engl J Med* 388 (2023): 1220-1221.
32. Bria A. Taking MRI to the next level of care with AI (2023). <https://blog.medicai.io/en/taking-mri-to-the-next-level-of-care-with-ai>. Accessed at 8/19/2023.
33. Rajput D, Wang WJ, Chen CC. Evaluation of a decided sample size in machine learning applications. *BMC Bioinformatics* 24 (2023): 48.